



# Synthesis of asymmetrical multiantennary human milk oligosaccharides

Anthony R. Prudden<sup>a,b</sup>, Lin Liu<sup>a</sup>, Chantelle J. Capicciotti<sup>a</sup>, Margreet A. Wolfert<sup>a,c</sup>, Shuo Wang<sup>a</sup>, Zhongwei Gao<sup>a</sup>, Lu Meng<sup>a</sup>, Kelley W. Moremen<sup>a</sup>, and Geert-Jan Boons<sup>a,b,c,d,e,1</sup>

<sup>a</sup>Complex Carbohydrate Research Center, University of Georgia, Athens, GA 30602; <sup>b</sup>Department of Chemistry, University of Georgia, Athens, GA 30602; <sup>c</sup>Department of Chemical Biology and Drug Discovery, Utrecht University, 3584 CG Utrecht, The Netherlands; <sup>d</sup>Utrecht Institute for Pharmaceutical Sciences, Utrecht University, 3584 CG Utrecht, The Netherlands; and <sup>e</sup>Bijvoet Center for Biomolecular Research, Utrecht University, 3584 CH Utrecht, The Netherlands

Edited by Chi-Huey Wong, Academia Sinica, Taipei, Taiwan, and approved May 25, 2017 (received for review February 1, 2017)

**Despite mammalian glycans typically having highly complex asymmetrical multiantennary architectures, chemical and chemoenzymatic synthesis has almost exclusively focused on the preparation of simpler symmetrical structures. This deficiency hampers investigations into the biology of glycan-binding proteins, which in turn complicates the biomedical use of this class of biomolecules. Herein, we describe an enzymatic strategy, using a limited number of human glycosyltransferases, to access a collection of 60 asymmetric, multiantennary human milk oligosaccharides (HMOs), which were used to develop a glycan microarray. Probing the array with several glycan-binding proteins uncovered that not only terminal glycoepitopes but also complex architectures of glycans can influence binding selectivity in unanticipated manners. N- and O-linked glycans express structural elements of HMOs, and thus, the reported synthetic principles will find broad applicability.**

chemoenzymatic synthesis | glycosyltransferases | protein–glycan interactions | human milk oligosaccharides

**H**uman breast milk is rich in a family of structurally diverse unconjugated glycans (1, 2). These compounds, which are the third largest component of breast milk, are not digested by the infant but serve as metabolic substrates for beneficial bacteria, thereby shaping the intestinal microbiome (3, 4). Human milk oligosaccharides (HMOs) also serve as soluble decoys for viral, bacterial, or protozoan parasite adhesins, thereby preventing attachment to the infant mucosal surface (5, 6). The fucosylated fraction of human milk, specifically structures containing H blood group epitopes, can inhibit *Campylobacter jejuni* colonization of mice in vivo and human intestinal mucosa ex vivo. HMOs can also modulate epithelial and immune cell responses and reduce excessive mucosal leukocyte infiltration and activation (7, 8). These properties have been associated with a lower risk for developing necrotizing enterocolitis (9).

Access to well-defined HMOs in sufficient quantity is a major obstacle for unraveling the biological mechanisms of action of these compounds and to exploit their biomedical potential (2, 10). Several simple HMOs are commercially available, and such compounds have been used in informative binding and biological studies (11, 12). Current strategies for obtaining more complex HMOs are cumbersome and rely on multidimensional chromatography of pooled breast milk (13) or laborious chemical or chemoenzymatic synthesis (14–22) that cannot provide the highly complex asymmetrical glycans found in human milk.

The structural complexity of HMOs ranges from relatively simple glycans, such as lactose and sialyl- and fucosyl-lactose, to highly complex, multibranching structures having different appendages at each branching point (Fig. 1 *A* and *B*) (1). All HMOs have a reducing lactose moiety that can be extended by various numbers of lacto-*N*-biose (Gal $\beta$ 1,3GlcNAc, type 1 LacNAc) or *N*-acetyllactosamine (Gal $\beta$ 1,4GlcNAc, type 2 LacNAc) motifs. Branched HMOs are formed by the action of *N*-acetylglucosaminyltransferase (GCNT2), which installs a  $\beta$ 1,6-linked *N*-acetylglucosamine (GlcNAc) at an internal galactosyl moiety that can be further extended by type 1 or

type 2 structures. Repeated action of GCNT2 creates highly complex, multiantennary structures. The termini of the resulting oligosaccharide chains can be modified by various combinations of  $\alpha$ 1,2-,  $\alpha$ 1,3-, and  $\alpha$ 1,4-fucosylation and  $\alpha$ 2,3- and  $\alpha$ 2,6-sialylation, providing an array of Lewis structures and blood group antigens (Fig. 1*B*). The resulting multiantennary HMOs often have asymmetrical architectures in which each appendage is modified by a unique glycoepitope.

We envisaged that the redundant nature of HMO biosynthesis would offer an avenue to create an array of structurally diverse symmetrically and asymmetrically branched HMOs by exploiting inherent substrate specificities of a limited number of mammalian glycosyltransferases. We anticipated that the penultimate galactoside of the linear tetrasaccharide lacto-*N*-neotetraose (LNnT) can be selectively modified by the I-branching enzyme GCNT2 to install a  $\beta$ 1,6-GlcNAc moiety providing an asymmetric pentasaccharide (Fig. 1*C*). The latter compound has terminal GlcNAc and LacNAc moieties, which can be selectively extended by exploiting the fact that most glycosyltransferases can modify a terminal LacNAc but not a GlcNAc residue. Thus, the  $\beta$ 3 antenna of the pentasaccharide can first be elaborated by a panel of glycosyltransferases, and at an appropriate stage of the synthesis, the terminal GlcNAc residue of the  $\beta$ 6 arm can be converted into LacNAc by the action of  $\beta$ 1,4-galactosyltransferase from bovine milk (GalT1). The newly formed LacNAc motif can then be further extended by various numbers of type 1 and type 2 structures, which in turn can be modified with different forms of fucosylation and/or sialylation to give highly complex, asymmetric, biantennary glycans. The process of installing a branching point using GCNT2 can be repeated on the newly

## Significance

**Human breast milk is rich in a family of structurally diverse unconjugated glycans. These human milk oligosaccharides (HMOs) can shape the intestinal microbiome, serve as soluble decoys for receptors of pathogens, and have immune-modulatory properties. Virtually nothing is known about the importance of the molecular complexity of HMOs for binding and biological activity, which hampers exploitation of their biomedical potential. We have developed a synthetic approach that can provide highly complex, asymmetrical, multiantennary HMOs. These compounds have been used in the development of a glycan microarray, which makes it possible to examine the biology of individual compounds. Binding studies with the array uncovered that the complex architecture of HMOs greatly affects protein–glycan binding.**

Author contributions: A.R.P., L.L., C.J.C., M.A.W., K.W.M., and G.-J.B. designed research; A.R.P., L.L., C.J.C., M.A.W., S.W., Z.G., and L.M. performed research; S.W., Z.G., and L.M. contributed new reagents/analytic tools; A.R.P., L.L., C.J.C., M.A.W., and G.-J.B. analyzed data; and A.R.P. and G.-J.B. wrote the paper.

The authors declare no conflict of interest.

This article is a PNAS Direct Submission.

<sup>1</sup>To whom correspondence should be addressed. Email: g.j.p.h.boons@uu.nl.

This article contains supporting information online at [www.pnas.org/lookup/suppl/doi:10.1073/pnas.1701785114/-DCSupplemental](http://www.pnas.org/lookup/suppl/doi:10.1073/pnas.1701785114/-DCSupplemental).

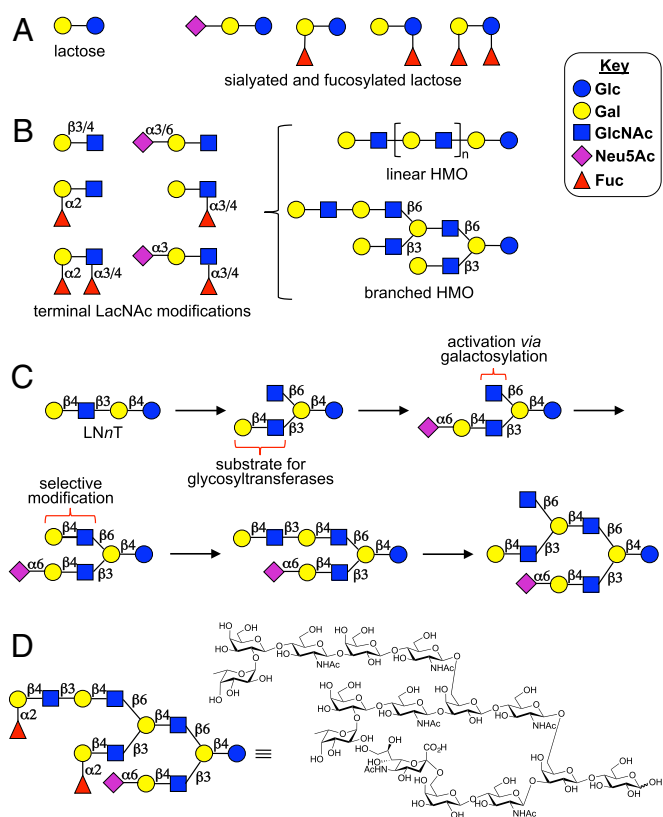


**Fig. 1.** Structural diversity of HMOs. (A) Simple HMOs. (B) Structural diversity of multiantennary HMOs. (C) Enzymatic strategy for the synthesis of asymmetric multiantennary HMOs. (D) Example of a chemical structure of an asymmetric multiantennary HMO prepared by the enzymatic approach.

extended  $\beta_6$  arm with subsequent galactosylation, branch extension, and finally selective fucosylation or sialylation to give entry into complex, asymmetric, triantennary glycans (Fig. 1D). The power of this strategy is demonstrated by the synthesis of a library of 60 linear, biantennary, and triantennary HMO structures, which were used to create a glycan microarray. Screening studies with several glycan binding proteins such as a galectin, a microbial toxin and a viral adhesion protein, uncovered that glycan complexity controls binding selectivity in unanticipated manners.

## Results and Discussion

**Synthesis of Asymmetric Biantennary HMOs.** Lactose, the reducing disaccharide of all HMOs, was modified with the multifunctional anomeric linker **1**, which was expected to have many attractive attributes (Fig. 2A; for the synthesis of **1**, see *SI Appendix, Fig. S1*). The *N*-methylhydroxylamine of **1** can selectively react with the reducing terminus of lactose (**2**) to provide the  $\beta$ -linked product **3** with retention of the pyranose ring (23). The hydrophobic coumarin moiety was expected to facilitate purification of synthetic intermediates by reverse phase column chromatography. Furthermore, the primary amine should facilitate compound immobilization onto *N*-hydroxysuccinimide (NHS) ester activated microarray slides for glycan array development (24). It also improves ionization of glycans during analysis by mass spectrometry. Finally, the anomeric linkage is acid labile, allowing its removal to provide reducing sugars.

The tetrasaccharide LNnT (**4**) was readily prepared by the subsequent treatment of **3** with  $\beta$ 1,3-*N*-acetylglucosaminyltransferase 2 (B3GNT2) in the presence of uridine-5'-diphospho (UDP)-GlcNAc and then with GalT1 and UDP-galactose (UDP-Gal; Fig. 2B). As anticipated, the enzyme GCNT2 modified only the penultimate galactoside of **4**, resulting in the formation of

asymmetric pentasaccharide **5**. The site of glycosylation was confirmed by NMR spectroscopy (*SI Appendix, Figs. S14–S17*), which showed a nuclear Overhauser effect (NOE) between H-1 ( $\delta$  4.44) of the  $\beta$ 1,6GlcNAc moiety and H-6 and H-6' ( $\delta$  3.81 and  $\delta$  3.64) of the internal Gal residue. Next, the LacNAc residue of **5** was sialylated using  $\alpha$ 2,6-sialyltransferase 1 (ST6GAL1) and cytidine-5'-monophospho-*N*-acetylneuraminic acid (CMP-Neu5Ac) to provide hexasaccharide **6**.

The progress of each enzymatic transformation was monitored by MALDI-TOF mass spectrometry (MS) without a need for chemical derivatization. Additional enzyme and sugar nucleotide were added if any starting material was observed. After each step, the product was purified by reverse phase column chromatography on C8 (e.g., *SI Appendix, Figs. S11–S13*), and the resulting compounds were fully characterized by NMR.

The next stage of synthesis involved elaboration of the  $\beta_6$  antenna of **6** by converting the terminal GlcNAc moiety into LacNAc with GalT1 and UDP-Gal to give **7** (Fig. 2B). Treatment of **7** with B3GNT2 and UDP-GlcNAc resulted in the selective addition of a  $\beta$ 1,3-GlcNAc moiety to LacNAc of the  $\beta_6$  antenna to provide glycan **8**, and subsequent treatment with GalT1 and UDP-Gal installed a second LacNAc motif to yield **9**. The  $\beta_3$  arm was unaffected because the  $\alpha$ 2,6-sialoside blocks modification by mammalian glycosyltransferases. Finally, an  $\alpha$ 1,2-fucoside was introduced to the terminal galactoside of **9** using galactoside  $\alpha$ 2-fucosyltransferase 1 (FUT1), an enzyme that only recognizes terminal type 1 or type 2 structures, to furnish decasaccharide **10** bearing an H2 epitope. The successful preparation of **10** highlights the feasibility of exploiting inherent substrate specificities of glycosyltransferases for the modification of

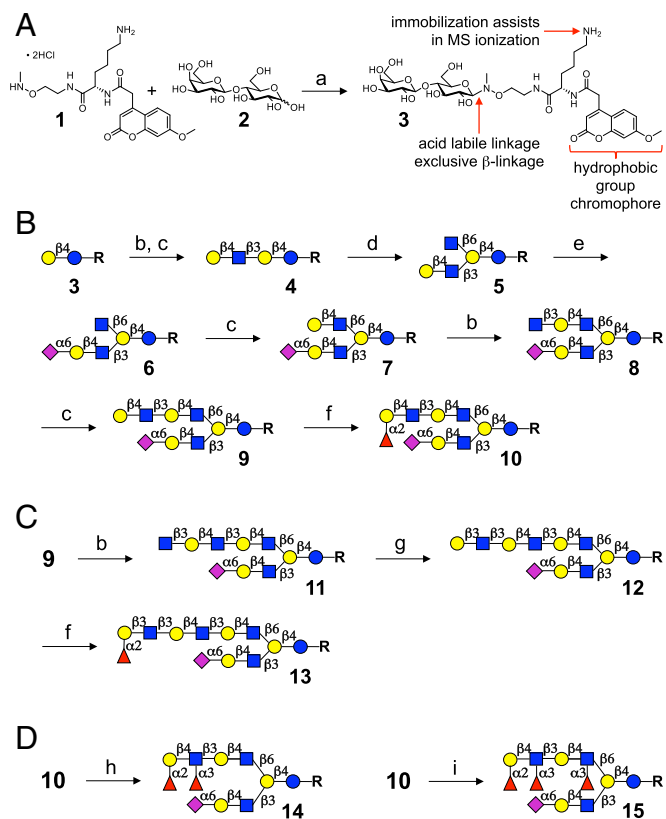


**Fig. 2.** Lactose linker conjugations and enzymatic synthesis of HMOs. (A) Lactose-linker complex. (B) Introducing structural asymmetry. (C) Extended poly-LacNAc  $\beta_6$  branch. (D) Selective fucosylation. Reagents and conditions: a, 0.25 M  $\text{CH}_3\text{CO}_2\text{Na}$ , pH 4.2, 37 °C; b, B3GNT2, UDP-GlcNAc; c, GalT1, UDP-Gal; d, GCNT2, UDP-GlcNAc; e, ST6GAL1, CMP-Neu5Ac; f, FUT1, GDP-Fuc; g, B3GALT5, UDP-Gal; h, FUT3, GDP-Fuc; and i, FUT5, GDP-Fuc.

multiantennary glycans in a branch selective manner. Advanced intermediate **9** could also be extended by a type 1 structure through the sequential action of B3GNT2 ( $\rightarrow$ **11**) and B3GALT5 to give **12** (Fig. 2C). The latter compound was treated with FUT1 to yield dodecasaccharide **13** having an H1 epitope at the terminus of a tri-LacNAc repeat on the  $\beta$ 6 arm. It was observed that B3GALT5 can readily galactosylate extended acceptors such as **11** to form a terminal type 1 structure; however, no observable addition occurred when shorter substrates such as glycans **6** or **8** were used.

**Selective Fucosylation.** An attractive feature of the motif-based enzymatic synthetic strategy is that advanced intermediates, such as **10** (Fig. 2B), can be modified by a panel of appropriate fucosyltransferases to install various types of blood group antigens, thereby creating considerable structural diversity. For example, mammalian lactosamine  $\alpha$ 1,3-4 fucosyltransferase 3 (FUT3) and 5 (FUT5) can both produce Lewis structures by adding  $\alpha$ 1,3- or  $\alpha$ 1,4-fucose to type 2 or type 1 structures, respectively. Despite high amino acid homology (91%), FUT5 preferentially forms  $\alpha$ 1,3- and FUT3  $\alpha$ 1,4-fucosides. However, when an acceptor bears an H2 epitope, FUT3 exhibits increased  $\alpha$ 1,3 reactivity to form a Lewis<sup>x</sup> (Le<sup>x</sup>) epitope (**25**). Taking advantage of these differences in reactivity, the H2 antigen of **10** could selectively be converted into a Le<sup>y</sup> epitope to give **14** by treatment with FUT3 and guanosine 5'-diphospho- $\beta$ -L-fucose (GDP-Fuc). Even after a prolonged reaction time and the presence of excess of GDP-Fuc, only one fucosyl residue was added, and an internal Le<sup>x</sup> moiety was not formed. In contrast, the use of FUT5 resulted in the addition of two fucosides providing a Le<sup>y</sup>-Le<sup>x</sup> motif to give glycan **15**.

Additional strategies were explored for controlling the site of fucosylation of glycans containing dimeric-LacNAc motifs. It is known that a terminal LacNAc moiety modified by an  $\alpha$ 2,6-sialoside cannot be fucosylated by FUT3 or FUT5, and therefore, it should be possible to selectively modify internal LacNAc residues. Subsequent removal of the sialoside by an appropriate sialidase would then provide uniquely fucosylated glycans. To demonstrate the feasibility of this strategy, biantennary glycan **16** was prepared by a similar strategy as described for compound **9** (SI Appendix, Fig. S8). Selective sialylation of the terminal galactoside of the  $\beta$ 6 arm of **16** by ST6GAL1 provided compound **17** (Fig. 3). The  $\beta$ 3 arm was unaffected by this sialyltransferase because the Le<sup>x</sup> epitope at the  $\beta$ 3 arm renders it inactive for modification by mammalian glycosyltransferases. As anticipated, treatment of **17** with FUT3 resulted in site-specific fucosylation of the internal LacNAc residue to give glycan **18**. Finally, the sialidase from *Arthrobacter ureafaciens* cleanly removes the sialoside of **18**, providing compound **19**.

It was anticipated that by combining inherent substrate specificities of fucosyltransferases with selective cleavage of terminal fucosides by a microbial fucosidase, entry into additional targets bearing a terminal Le<sup>x</sup> epitope could be achieved. For example, FUT3 preferentially modifies H2 epitopes, and therefore,

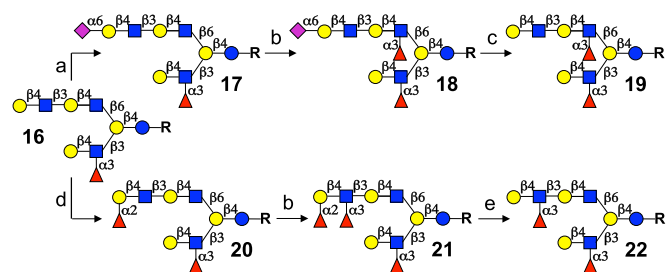


**Fig. 3.** Monosaccharide directing groups for selective Le<sup>x</sup> installation. Reagents and conditions: a, ST6GAL1, CMP-Neu5Ac; b, FUT3, GDP-Fuc; c, sialidase from *Arthrobacter ureafaciens*; d, FUT1, GDP-Fuc; and e, microbial  $\alpha$ 1-2 fucosidase.

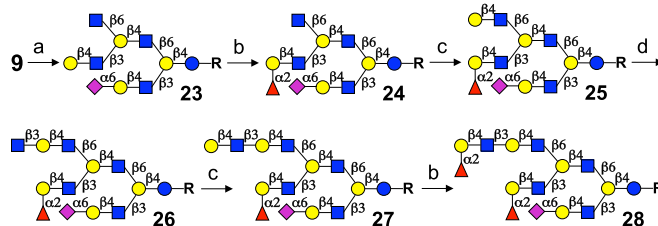


**Fig. 4.** Synthesis of an asymmetric, triantennary HMO. Reagents and conditions: a, GCNT2, UDP-GlcNAc; b, FUT1, GDP-Fuc; c, GalT1, UDP-Gal; and d, B3GNT2, UDP-GlcNAc.

exposure of **20** to this enzyme resulted in the selective formation of a Le<sup>y</sup> epitope to give compound **21**. The sites of fucosylation were confirmed by NMR spectroscopy using chemical shift and NOE analysis (SI Appendix, Figs. S18–S21). The terminal  $\alpha$ 1,2-fucoside of **21** could be cleaved without affecting any of the other fucosides by using a microbial fucosidase having  $\alpha$ 1,2 selectivity resulting in the clean formation of **22**. These results demonstrate that unique glycan architectures can be created by combining the inherent regioselectivities of glycosyltransferases with glycosidases that hydrolyze specific glycoepitopes.

**Synthesis of Asymmetric Triantennary HMOs.** The final challenge was to expand the methodology to the synthesis of asymmetrical, triantennary glycans such as **28**. It was anticipated that the process of installing a second branching point using GCNT2, followed by galactosylation, elaboration with various numbers of LacNAc repeating units, and finally fucosylation or sialylation, could be performed on biantennary glycans to give entry into asymmetrical triantennary structures. Thus, starting from advanced intermediate **9**, GCNT2 selectively installed a  $\beta$ 6-GlcNAc on the internal LacNAc of the  $\beta$ 6 arm to furnish decasaccharide **23** (Fig. 4). Treatment of **23** with FUT1 resulted in  $\alpha$ 1,2-fucosylation of the LacNAc moiety of the middle  $\beta$ 3-branch leading to the formation of an H2 epitope while leaving the  $\beta$ 6-GlcNAc branching moiety unmodified (compound **24**). The terminal fucose (H2 antigen) prevented any further extension of the middle  $\beta$ 3 branch with LacNAc repeating units, and therefore, the  $\beta$ 6 arm could be exclusively elongated by the sequential application of GalT1 ( $\rightarrow$ **25**), B3GNT2 ( $\rightarrow$ **26**), and GalT1 to provide tetradecasaccharide **27**. Finally, fucosylation of **27** with FUT1 furnished asymmetric pentadecasaccharide **28**, which is endowed with two H2 epitopes and a 6'-sialyl-LacNAc motif.

**Construction of an HMO Glycan Microarray.** To demonstrate the versatility of the methodology, a library of 60 linear, biantennary, and triantennary HMOs was prepared (Fig. 5; for synthesis, see Figs. 2–4 and SI Appendix, Figs. S2–S9), which were printed onto NHS ester activated glass slides to create an HMO glycan microarray. The resulting slides were examined for binding to the plant lectins *Sambucus nigra* agglutinin (SNA), *Ulex europaeus* agglutinin I (UEA), and *Aleuria aurantia* (AAL), which recognize  $\alpha$ 2,6-sialosides;  $\alpha$ 1,2-fucosides; and  $\alpha$ 1,2-  $\alpha$ 1,3-, and  $\alpha$ 1-6 fucosides, respectively. These studies confirmed spot integrity and proper substrate deposition (SI Appendix, Fig. S22).

We next examined recognition of the glycans on the microarray by a number of glycan binding proteins whose activity may be modulated by HMOs including Galectin 9 (Gal-9) (**26**), the AB<sub>5</sub> toxin of *Vibrio cholera*, and a rotaviral adhesion protein (Fig. 6). Galectins are a family of  $\beta$ -galactoside binding proteins that are involved in a number of physiological and disease processes including immune modulation (**27**). Previous studies have shown that Gal-9 can bind type 1 and type 2 LacNAc structures with a preference for extended chains (**28**, **29**). Furthermore, the presence of a terminal  $\alpha$ 2,3-sialoside or  $\alpha$ 1,3/4-fucoside abolishes binding. HMOs on the array that exhibited moderate to strong responsiveness to Gal-9 all possessed an extended LacNAc motif on the  $\beta$ 6 arm, which probably is the main site of

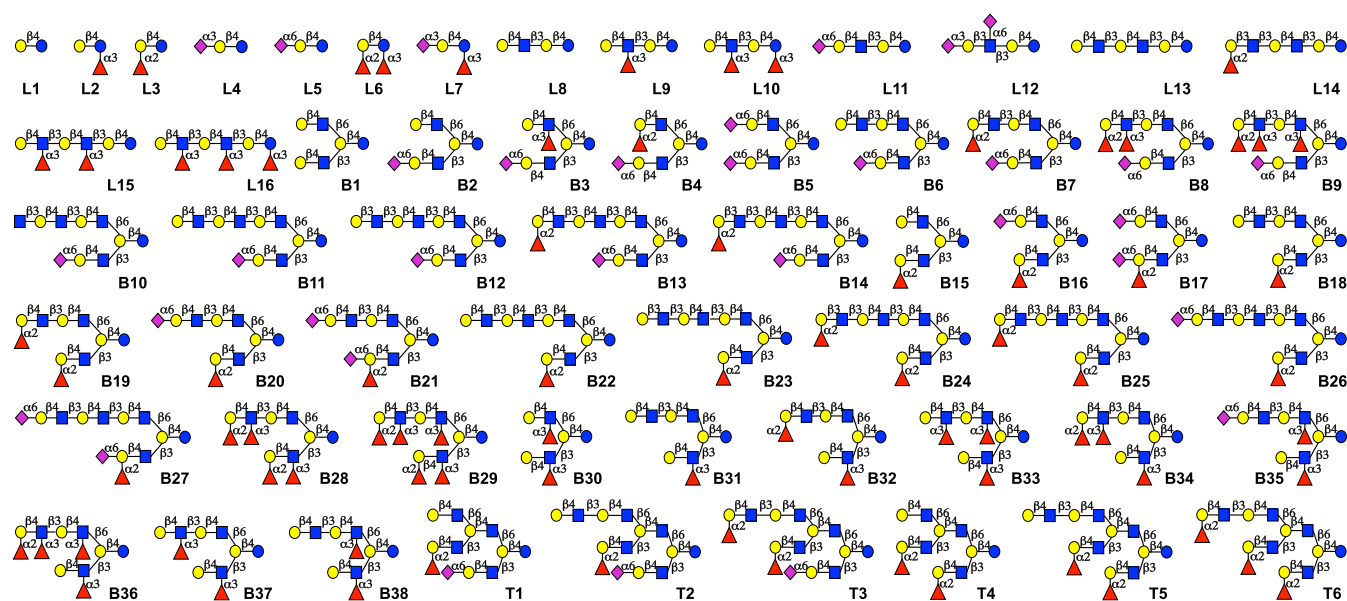


Fig. 5. HMO library members. The compounds are organized according to an increase in complexity. B, biantennary glycan; L, linear glycan; and T, triantennary glycan. See *SI Appendix, Table S2*, for correlation of library identifier with compound synthesis number.

binding (Fig. 6A). The presence of a terminal type 1 structure resulted in substantially stronger binding (**B23** vs. **B22**). An  $\alpha$ 2,6-sialoside capping a trimeric LacNAc moiety at the  $\beta$ 6 arm also increased responsiveness (**B26** vs. **B22**), whereas a similar modification of dimeric LacNAc abolished binding (**B20** vs. **B18**). Terminal  $\alpha$ 1,2-fucosylation on the  $\beta$ 6 arm provided an H-antigen that reduced or abolished binding (**B19** vs. **B18**, **B25** vs. **B22**, and **B24** vs. **B23**). Other forms of fucosylation of the  $\beta$ 6 arm were also not tolerated for Gal-9 binding. The glycan epitope of the  $\beta$ 3 antenna greatly influenced binding of an extended LacNAc motif on the  $\beta$ 6 arm. For example, the presence of an H2 epitope on the  $\beta$ 3 arm was tolerated (**B18**, **B23**, and **B24**), whereas an  $\alpha$ 2,6-sialoside abolished binding (compared with **B6**, **B12**, and **B14**, respectively). A similar result was obtained with the triantennary HMOs where binding was observed when the bottom  $\beta$ 3 antenna bears an H2 epitope but is not detected when this site contained an  $\alpha$ 2,6-sialoside (**T5** vs. **T2**). Furthermore, a Le<sup>x</sup> moiety on the  $\beta$ 3 arm rather than an H2 was also detrimental for binding (**B31** vs. **B18**). Even sialylation of the  $\beta$ 3 arm of compound **B26** to give **B27** resulted in a loss of interaction.

Next, binding properties of the B<sub>5</sub> subunit of the AB<sub>5</sub> toxin *V. cholera* were explored (Fig. 6B). This pentameric protein facilitates cell adhesion and permits endocytosis of the toxic A subunit. It recognizes with high affinity the ganglioside GM1 (30); however, recent studies have demonstrated that it can also bind fucosylated glycans of glycoproteins (31). The two compounds on the microarray that showed the greatest responsiveness have asymmetrical architectures bearing Le<sup>y</sup> epitopes at the  $\beta$ 3 and  $\beta$ 6 branch (**B28** and **B29**). Compounds that displayed only one Le<sup>y</sup> epitope (**B8** and **B9**) showed no binding. Even removal of only a single fucosyl residue to give Le<sup>x</sup> on the  $\beta$ 3 antenna, while maintaining the presence of a  $\beta$ 6 Le<sup>y</sup> epitope, substantially reduced binding (**B34** and **B36**). These observations highlight that the complex architecture of HMOs modulate binding and indicate that a bivalent interaction of the toxin with Le<sup>y</sup> at the  $\beta$ 3 and  $\beta$ 6 arm results in increased avidity.

As a third class of glycan binding proteins that interacts with HMOs, we explored the binding selectivity of an adhesion protein from a rotavirus. These viruses cause viral gastroenteritis and diarrhea in infants and the young of various animal species. Infectivity requires that the surface viral spike protein VP4 be cleaved into VP5\* and VP8\* fragments, where the latter is responsible for cellular adhesion (32). The porcine strain CRW-8

has been termed “sialidase sensitive” because infectivity requires sialic acid for adhesion and subsequent infection. Recently, it was demonstrated that VP8\* of CRW-8 recognizes the glycolipid aceramido-GM3, which is composed of an  $\alpha$ 2,3-sialoside linkage to lactose (33, 34). The HMO microarray is sparsely populated with  $\alpha$ 2,3-sialosides, which showed no interaction with VP8\* (Fig. 6C). The compounds that exhibited strong responsiveness (**B2**, **B6**, **B11**, **T1**, and **T2**) have asymmetric architectures displaying a  $\alpha$ 2,6-sialylLacNAc moiety at the  $\beta$ 3 antenna and a terminal type 2 LacNAc residue on the  $\beta$ 6 branch. Compounds that lack the latter residue, such as **B3**, **B4**, **B5**, **B7**, **B8**, **B10**, and **B13**, but maintain an  $\alpha$ 2,6-sialylLacNAc at the  $\beta$ 3 arm were not recognized by the protein. A terminal type 1 structure, such as in compound **B12**, was also not tolerated (compared with **B11**). Triantennary HMOs that display a terminal  $\alpha$ 2,6-sialylLacNAc on the lower  $\beta$ 3 arm and terminal LacNAc motifs on the upper  $\beta$ 6 arm also showed strong responsiveness to VP8\* (**T1** and **T2**). In these cases, the presence of an H2 epitope on the middle  $\beta$ 3 arm did not interfere with binding, whereas an H2 moiety on the lower and middle  $\beta$ 3 arms abolished any interaction with the protein (**T4** and **T5**). These results suggest that high binding avidity is accomplished through heteromultivalency in which a bivalent interaction is established with two different binding sites having different ligand requirements.

## Conclusion

The ultimate challenge in infant nutrition is to make formula derived from bovine milk with increased similarity to human milk in terms of composition and functionality. HMOs represent a broad pool of glycan structures that are mostly absent in bovine milk but have a wide range of antimicrobial effects against pathogens that cause diarrhea, as well as regulating the immune system and intestinal physiology. Supplementation with key human milk glycans is beginning to take root as the European Food Safety Authority reported that 2'-O-fucosyllactose is safe to be used as a human food additive (35). There is also a realization that HMOs have potential for medical purposes such as lowering the risk of developing necrotizing enterocolitis in neonates (9). Despite these promises, the relationship between HMO structures and biological activity remains largely unknown due to a lack of well-defined compounds, especially those that have complex architectures. Cummings and coworkers developed a glycan microarray by fractionation of human milk by multidimensional

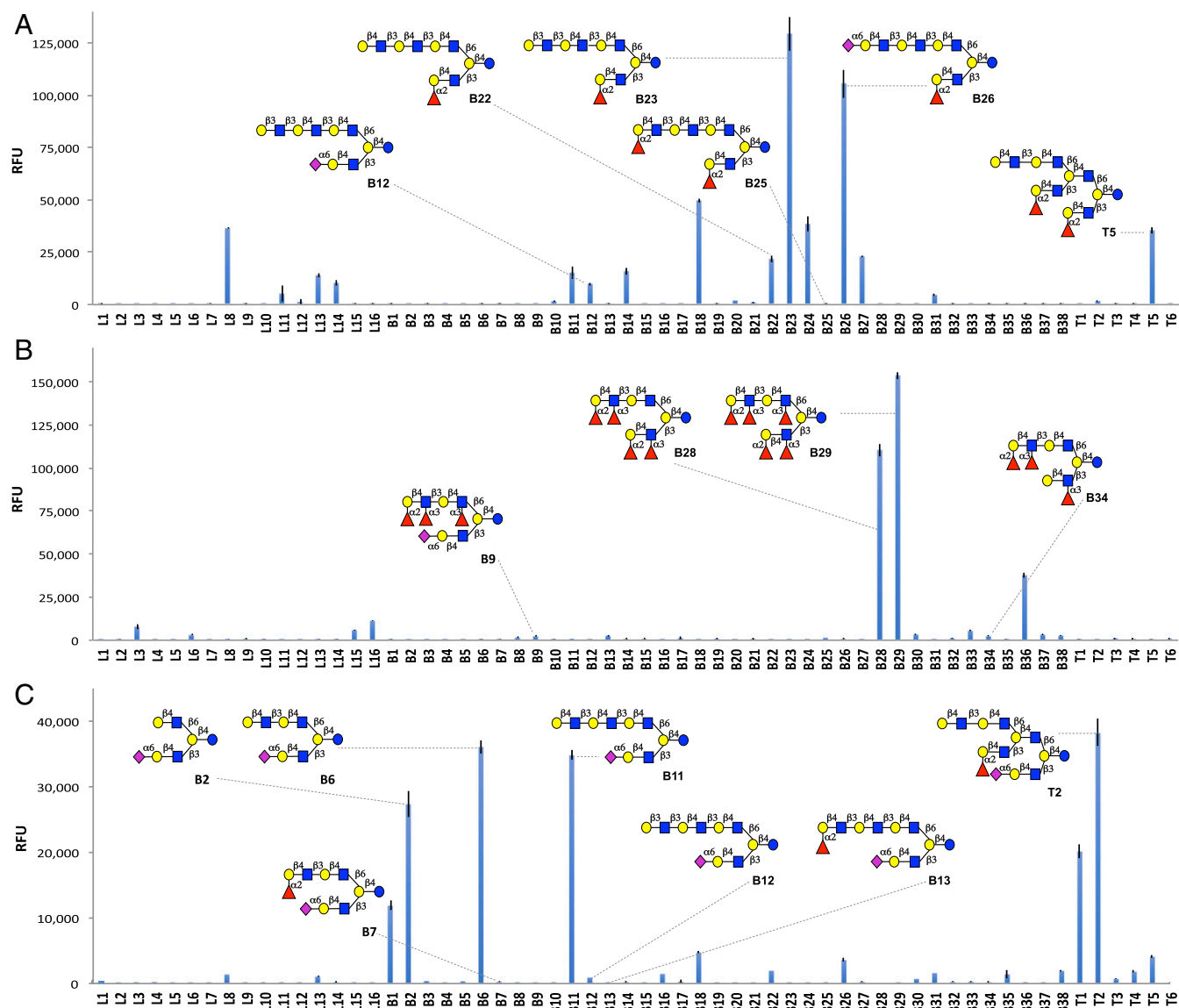


**Fig. 6.** Screening of the HMO library. Microarray results of the HMO library at 100  $\mu\text{M}$ . (A) Galectin-9 ( $3 \mu\text{g}\cdot\text{mL}^{-1}$ ). (B) *V. cholera* toxin subunit B<sub>5</sub> ( $100 \mu\text{g}\cdot\text{mL}^{-1}$ ). (C) Porcine rotaviral strain CRW-8 VP8\* ( $200 \mu\text{g}\cdot\text{mL}^{-1}$ ). RFU, relative fluorescence units.

chromatography followed by chemical modification for immobilization to glass slides (36, 37). Despite attractive features, such a shotgun approach suffers from difficulties of structure identification of active compounds, false positive hits due to insufficient compound purification, and problems in follow-up studies due to lack of sufficient quantities of material. A number of HMOs have been synthesized (14–22); however, the methods used can only provide molecules with relatively simple architectures. The synthetic strategy described here addresses these deficiencies and can provide entry into a wide array of highly complex HMOs. Strategically desymmetrizing selected oligosaccharides by installing a branching point through the action of the GCNT2 enzyme created the opportunity to systematically build complex, asymmetric HMOs. Exploiting inherent substrate specificities of glycosyltransferases and hydrolases yielded a library representing compounds of enormous structural diversity. This current synthetic strategy is different from the previously reported approach for preparing asymmetric N-glycans (38), which relied on a chemically prepared, orthogonally protected, core pentasaccharide. The current methodology was used to prepare a library of 60 linear, biantennary, and triantennary glycans, which were used for the development of a

microarray. Binding studies with three glycan binding proteins revealed that the topology of HMOs greatly influences recognition, possibly through homomultivalent and heteromultivalent interactions or negative allosteric modulation by neighboring glycan branches. It is widely accepted that terminal oligosaccharide motifs of complex glycans mediate biological recognition (39, 40); however, the results presented here show that complex glycan architecture modulates binding in unanticipated manners.

## Materials and Methods

Full experimental details and characterization of the compounds are given in *SI Appendix*.

**General Materials and Methods for Enzymatic Synthesis.** Enzymatic reactions were incubated overnight at  $37^\circ\text{C}$  with gentle shaking. Reaction progress was monitored by MALDI-TOF MS using 2,5-dihydroxybenzoic acid (DHB) as a matrix. If starting material was detected after 18 h, a second portion of enzyme was added. When no starting material was detected, enzymes and BSA were removed by centrifugation using a Nanosep Omega ultrafiltration device (10 kDa cut off). The filtrate was lyophilized, and products were purified by reverse-phase HPLC (*SI Appendix*). GalT1 from bovine milk was purchased from

Sigma. Sialidase from *Arthrobacter ureafaciens* was purchased from Roche, and 1,2- $\alpha$ -L-fucosidase (microbial) was purchased from Megazyme.

**Procedure for the Installation of  $\beta$ 1,3 GlcNAc (8, 11, 26).** HMO (7, 9 or 25) and UDP-GlcNAc (1.5 eq per GlcNAc added) were dissolved at a final HMO concentration of 10 mM in a HEPES buffer (50 mM, pH 7.3) containing KCl (25 mM), MgCl<sub>2</sub> (2 mM), and DTT (1 mM). To this mixture, calf intestine alkaline phosphatase (CIAP, 10 U  $\mu$ L<sup>-1</sup>) and B3GNT2 (8.3  $\mu$ g per  $\mu$ mol HMO) were added. Following purification, the respective products (8, 87%; 11, 82%; and 26, 85%) were obtained as white solids.

**Procedure for the Installation of Branching  $\beta$ 1,6 GlcNAc (5, 23).** HMO (4 or 9) and UDP-GlcNAc (1.5 eq per GlcNAc added) were dissolved at a final HMO concentration of 10 mM in a MES buffer (50 mM, pH 7.0) containing Na<sub>2</sub>EDTA (10 mM). To this mixture, CIAP (10 U  $\mu$ L<sup>-1</sup>) and GCNT2 (7.5  $\mu$ g per  $\mu$ mol HMO) were added. Following purification, the respective products (5, 78%, and 23, 74%) were obtained as white solids.

**Procedure for the Installation of  $\beta$ 1,4 Gal to Form Type II LacNAc Moieties (7, 9, 25, 27).** HMO (6, 8, 24, or 26) and UDP-Gal (1.5 eq per Gal added) were dissolved at a final HMO concentration of 10 mM in a Tris buffer (50 mM, pH 7.3) containing MnCl<sub>2</sub> (10 mM) and BSA (0.1% wt/wt). To this mixture, CIAP (10 U  $\mu$ L<sup>-1</sup>) and GalT1 (5  $\mu$ g per  $\mu$ mol HMO) were added. Following purification, the respective products (7, 90%; 9, 92%; 25, 88%; and 27, 85%) were obtained as white solids.

**Procedure for the Installation of  $\beta$ 1,3 Gal to Form Type I LacNAc Moieties (12).** HMO 11 and UDP-Gal (1.5 eq per Gal added) were dissolved at a final HMO concentration of 10 mM in a sodium cacodylate buffer (150 mM, pH 7.5) containing MnCl<sub>2</sub> (10 mM) and BSA (0.1% wt/wt). To this mixture, CIAP (10 U  $\mu$ L<sup>-1</sup>) and B3GALT5 (8.2  $\mu$ g per  $\mu$ mol HMO) were added. Following purification, compound 12 (80%) was obtained as a white solid.

**Procedure for the Installation of  $\alpha$ 1,2 Fuc (10, 13, 20, 24, 28).** HMO (9, 12, 16, 23, or 27) and GDP-Fuc (1.5 eq per Fuc added) were dissolved at a final

HMO concentration of 10 mM in a Tris buffer (50 mM, pH 7.3) containing MnCl<sub>2</sub> (10 mM). To this mixture, CIAP (10 U  $\mu$ L<sup>-1</sup>) and FUT1 (10  $\mu$ g per  $\mu$ mol HMO) were added. Following purification, the respective products (10, 90%; 13, 93%; 20, 88%; 24, 87%; and 28, 90%) were obtained as white solids.

**Procedure for the Installation of  $\alpha$ 1,3 Fuc Using FUT3 (14, 18, 21).** HMO (10, 17, or 20) and GDP-Fuc (1.5 eq per Fuc added) were dissolved at a final HMO concentration of 10 mM in a Tris buffer (50 mM, pH 7.3) containing MnCl<sub>2</sub> (10 mM). To this mixture, CIAP (10 U  $\mu$ L<sup>-1</sup>) and FUT3 (10  $\mu$ g per  $\mu$ mol HMO) were added. Following purification, the respective products (14, 86%; 18, 85%; and 21, 90%) were obtained as white solids.

**Procedure for the Installation of  $\alpha$ 1,3 Fuc Using FUT5 (15).** HMO 10 and GDP-Fuc (1.5 eq per Fuc added) were dissolved at a final HMO concentration of 10 mM in a Tris buffer (50 mM, pH 7.3) containing MnCl<sub>2</sub> (10 mM). To this mixture, CIAP (10 U  $\mu$ L<sup>-1</sup>) and FUT5 (10  $\mu$ g per  $\mu$ mol HMO) were added. Following purification, compound 15 (81%) was obtained as a white solid.

**Procedure for the Installation of Terminal  $\alpha$ 2,6 Neu5Ac (6, 17).** HMO (5 or 16) and CMP-Neu5Ac (1.5 eq per Neu5Ac) were dissolved at a final HMO concentration of 10 mM in a sodium cacodylate buffer (100 mM, pH 6.5) containing BSA (0.1% wt/wt). To this mixture, CIAP (10 U  $\mu$ L<sup>-1</sup>) and ST6GAL1 (4.4  $\mu$ g per  $\mu$ mol HMO) were added. Following purification, the respective products (6, 96%, and 17, 89%) were obtained as white solids.

**ACKNOWLEDGMENTS.** This research was supported by the National Institute of General Medical Sciences (R01GM090269 and P01GM107012 to G.-J.B. and P41GM103390 to K.W.M.); the National Heart, Lung, and Blood Institute (P01HL107150 to G.-J.B.); and the National Cancer Institute (F31CA180478 to A.R.P.) from the US National Institutes of Health (NIH). The research benefitted from instrumentation provided by NIH Grant S10RR027097. The content is solely the responsibility of the authors and does not necessarily represent the official views of the NIH.

- Kunz C, Rudloff S, Baier W, Klein N, Strobel S (2000) Oligosaccharides in human milk: Structural, functional, and metabolic aspects. *Annu Rev Nutr* 20:699–722.
- Bode L (2012) Human milk oligosaccharides: Every baby needs a sugar mama. *Glycobiology* 22:1147–1162.
- Charbonneau MR, et al. (2016) A microbial perspective of human developmental biology. *Nature* 535:48–55.
- Subramanian S, et al. (2015) Cultivating healthy growth and nutrition through the gut microbiota. *Cell* 161:36–48.
- Kunz C, Rudloff S (2008) Potential anti-inflammatory and anti-infectious effects of human milk oligosaccharides. *Bioactive Components of Milk*, Advances in Experimental Medicine and Biology, ed Böse Z (Springer, New York), Vol 606, pp 455–466.
- Etzold S, Bode L (2014) Glycan-dependent viral infection in infants and the role of human milk oligosaccharides. *Curr Opin Virol* 7:101–107.
- Newburg DS, Walker WA (2007) Protection of the neonate by the innate immune system of developing gut and of human milk. *Pediatr Res* 61:2–8.
- Kulinich A, Liu L (2016) Human milk oligosaccharides: The role in the fine-tuning of innate immune responses. *Carbohydr Res* 432:62–70.
- Jantscher-Krenn E, et al. (2012) The human milk oligosaccharide disialyllacto-N-tetraose prevents necrotizing enterocolitis in neonatal rats. *Gut* 61:1417–1425.
- Chichlowski M, German JB, Lebrilla CB, Mills DA (2011) The influence of milk oligosaccharides on microbiota of infants: Opportunities for formulas. *Annu Rev Food Sci Technol* 2:331–351.
- Shang J, et al. (2013) Identifying human milk glycans that inhibit norovirus binding using surface plasmon resonance. *Glycobiology* 23:1491–1498.
- Noll AJ, et al. (2016) Human DC-SIGN binds specific human milk glycans. *Biochem J* 473:1343–1353.
- Yu Y, et al. (2012) Functional glycomic analysis of human milk glycans reveals the presence of virus receptors and embryonic stem cell biomarkers. *J Biol Chem* 287:44784–44799.
- Takamura T, Chiba T, Ishihara H, Tejima S (1980) Chemical modification of lactose. 13. Synthesis of lacto-N-tetraose. *Chem Pharm Bull (Tokyo)* 28:1804–1809.
- Takamura T, Chiba T, Tejima S (1981) Chemical modification of lactose. 16. Synthesis of lacto-N-neohexaose. *Chem Pharm Bull (Tokyo)* 29:587–590.
- Knurr P, Castro-Palominio J, Grathwohl M, Schmidt RR (2001) Complex structures of antennary human milk oligosaccharides - Synthesis of a branched octasaccharide. *Eur J Org Chem* 2001:4239–4246.
- Roussel F, Takhi M, Schmidt RR (2001) Solid-phase synthesis of a branched hexasaccharide using a highly efficient synthetic strategy. *J Org Chem* 66:8540–8548.
- Jennum CA, Fenger TH, Bruun LM, Madsen R (2014) One-pot glycosylations in the synthesis of human milk oligosaccharides. *Eur J Org Chem* 2014:3232–3241.
- Yu H, et al. (2014) Synthetic disialyl hexasaccharides protect neonatal rats from necrotizing enterocolitis. *Angew Chem Int Ed Engl* 53:6687–6691.
- Chen C, et al. (2015) Sequential one-pot multienzyme (OPME) synthesis of lacto-N-neotetraose and its sialyl and fucosyl derivatives. *Chem Commun (Camb)* 51:7689–7692.
- Yao W, Yan J, Chen X, Wang F, Cao H (2015) Chemoenzymatic synthesis of lacto-N-tetrasaccharide and sialyl lacto-N-tetrasaccharides. *Carbohydr Res* 401:5–10.
- Xiao Z, et al. (2016) Chemoenzymatic synthesis of a library of human milk oligosaccharides. *J Org Chem* 81:5851–5865.
- Peri F, Dumy P, Mutter M (1998) Chemo- and stereoselective glycosylation of hydroxylamine derivatives: A versatile approach to glycoconjugates. *Tetrahedron* 54:12269–12278.
- Rillahan CD, Paulson JC (2011) Glycan microarrays for decoding the glycome. *Annu Rev Biochem* 80:797–823.
- Kannagi R (2014) Fucosyltransferase 5. GDP-fucose lactosamine  $\alpha$ 3/4-fucosyltransferase (FUT5). *Handbook of Glycosyltransferases and Related Genes*, eds Taniguchi N, et al. (Springer, Tokyo), pp 549–558.
- Rabinovich GA, Toscano MA (2009) Turning 'sweet' on immunity: Galectin-glycan interactions in immune tolerance and inflammation. *Nat Rev Immunol* 9:338–352.
- de Kivit S, et al. (2012) Galectin-9 induced by dietary synbiotics is involved in suppression of allergic symptoms in mice and humans. *Allergy* 67:343–352.
- Sato M, et al. (2002) Functional analysis of the carbohydrate recognition domains and a linker peptide of galectin-9 as to eosinophil chemoattractant activity. *Glycobiology* 12:191–197.
- Hirabayashi J, et al. (2002) Oligosaccharide specificity of galectins: A search by frontal affinity chromatography. *Biochim Biophys Acta* 1572:232–254.
- Kim CS, Seo JH, Cha HJ (2012) Functional interaction analysis of GM1-related carbohydrates and *Vibrio cholerae* toxins using carbohydrate microarray. *Anal Chem* 84:6884–6890.
- Wands AM, et al. (2015) Fucosylation and protein glycosylation create functional receptors for cholera toxin. *eLife* 4:e09545.
- Méndez E, López S, Cuadras MA, Romero P, Arias CF (1999) Entry of rotaviruses is a multistep process. *Virology* 263:450–459.
- Haselhorst T, et al. (2009) Sialic acid dependence in rotavirus host cell invasion. *Nat Chem Biol* 5:91–93.
- Yu X, et al. (2011) Novel structural insights into rotavirus recognition of ganglioside glycan receptors. *J Mol Biol* 413:929–939.
- EFSA Panel on Dietetic Products, Nutrition and Allergies (2015) Safety of 2'-O-fucosylactose as a novel food ingredient pursuant to Regulation (EC) No 258/97. *EFSA J* 13:4184.
- Ashline DJ, et al. (2014) Structural characterization by multistage mass spectrometry (MSn) of human milk glycans recognized by human rotaviruses. *Mol Cell Proteomics* 13:2961–2974.
- Yu Y, et al. (2014) Human milk contains novel glycans that are potential decoy receptors for neonatal rotaviruses. *Mol Cell Proteomics* 13:2944–2960.
- Wang Z, et al. (2013) A general strategy for the chemoenzymatic synthesis of asymmetrically branched N-glycans. *Science* 341:379–383.
- Varki A (2007) Glycan-based interactions involving vertebrate sialic-acid-recognizing proteins. *Nature* 446:1023–1029.
- Taylor ME, Drickamer K (2009) Structural insights into what glycan arrays tell us about how glycan-binding proteins interact with their ligands. *Glycobiology* 19:1155–1162.